Continuum electron emission from collisions of 0.1–3.2-MeV Kr ions with Kr and Xe targets

P. Clapis and Q. C. Kessel
Department of Physics and the Institute of Materials Science, University of Connecticut, Storrs, Connecticut 06268
(Received 22 January 1990)

The electron emission spectra observed following collisions of heavy ions with heavy atoms is often dominated by electrons with a continuous range of energies. The impact-parameter dependence for the emission of these electrons from Kr-Kr and Kr-Xe collisions has been measured for collision energies from 0.1 to 3.2 MeV and for scattering angles from 3° to 10° by measuring the emitted electrons in coincidence with the scattered ions. These data indicate that most of the ionization (often 20 to 25 electrons from the collision system) resulting from these heavy-ion–atom collisions occurs during the collision on a time scale of 10^{-16}–10^{-17} sec, as opposed to Auger decay in the separated atoms following the collision. For each combination thresholds were observed for electron production as a function of the collision's distance of closest approach. These excitation thresholds agree well with promoted molecular orbitals calculated within the framework of the Fano-Lichten model and indicate that this model is useful beyond its expected range of applicability.

I. INTRODUCTION

The energy spectra of electrons ejected when heavy ions collide with heavy atoms differ from the corresponding spectra observed with lighter ions where well-defined electron peaks are usually observed. For the heavier systems the spectra are often dominated by a continuum distribution of electrons and any well-defined peaks from autoionization of outer shells or Auger ionization of inner shells, if they are observed at all, appear as small peaks on top of this continuum. Gordeev and Woerlee and coworkers were the first to study the continuum electrons from Kr-Kr collisions[1,2] and they interpreted their results within the framework of the molecular orbital (MO) model proposed by Fano and Lichten.[3,4] They divided the continuum into two parts and suggested a different excitation mechanism for each: The higher-energy portion of the spectrum (above 300 eV) they attributed to direct coupling of highly excited MO's with the continuum and the lower-energy portion was attributed to the filling of the $4p\pi$ MO during the collision. Liesen and co-workers[5] used an electron-ion coincidence technique to measure the impact-parameter dependence of electrons from Kr^{4+}-Kr collisions. They observed a slight oscillation superimposed on the continuum and found it consistent with the possibility of interference between the filling of the $4p$ MO on the incoming and outgoing portions of the trajectory; however, attempts to repeat these data have not been successful.[6,7] Afrosimov and coworkers have also used the coincidence technique to study the continuum observed following 5–50-keV collisions of O, Ne, and Kr ions with similar targets.[8] They report appreciable cross sections for quasimolecular Auger transitions and find their data to be consistent with the model proposed by Liesen and co-workers and a theoretical calculation by Fricke and Sepp.[9] However, the present coincidence data indicate that molecular orbitals other than the $4p\pi$ MO provide the excitation mechanism in these collisions. It is not yet clear exactly what processes do result in the high final charge states (10 to 15 times ionized[10]), although the data of deGroot and co-workers[11–13] show that Auger processes occurring in the separated atoms following the collision are responsible for less than 10% of the ionization.

Electrons from the lighter Ar-Ar system at collision energies from 150 to 300 keV have been studied by Schiwietz and co-workers[14] with an innovative time-of-flight technique which provides the impact parameter dependence of the electron emission. They observe electrons with a continuous range of energies, but below the energy at which the Ar L Auger electrons are observed. They find the intensities of the continuous portion of the spectra to be approximately equal to the Auger intensities. They attribute these lower-energy electrons to the promotion of $4f\sigma$ electrons directly into the continuum. This interpretation is in contrast with the results of a lower-energy investigation of the same system[15,16] where it was found that at the threshold for L-shell excitation the promotion of a $4f\sigma$ electron resulted in an increase in ionization of only 1.3 units of charge. (That is, the promoted electron is not generally removed from the system at lower velocities.) Other sources which Schiwietz and co-workers considered to be less likely sources of continuum electrons for the Ar-Ar system included shakeoff, three-electron Auger processes, and Auger decay of the quasimolecule during the collision. Quasimolecular x-ray emission, analogous to this last process, has been studied extensively and a review of this work has been published by Anholt.[17]

This paper presents data from Kr-Kr and Kr-Xe collisions for collision energies from 0.1 to 3.2 MeV. Noncoincident measurements of the electron spectra show a broad electron continuum extending to energies greater than 1 keV. Of particular interest is the range from 100

to 600 eV where clear shoulders are observed in the spectra. Electron-ion coincidence measurements were performed for ion scattering angles from 3° to 10°. These latter data show distinct thresholds for excitation when the data are plotted versus the collision's distance of closest approach R_0. This feature of the data is like that reported in earlier ionization and inelastic energy-loss measurements;[10] however, those data could only infer that the features observed might be due to excitation of certain shells. The present coincidence technique now allows the association of a specific electron energy with a known R_0 and provides new insights into both the ionization mechanisms important here and the molecular orbital model. Preliminary reports have been made of these data,[18,19] and the thresholds observed provide evidence that certain aspects of the MO model may be used to explain electron excitation for R_0 values and binding energies for which the model was not originally intended. The excitations observed here are not associated with the innermost electron shells but with the more loosely bound outer shells. The MO model is an independent-electron approximation based on the assumption that each electron moves in a potential due to the two nuclei screened by the other electrons. For inner-shell electrons the dominant interaction is with the strong nuclear charge and the independent-electron approximation has enjoyed great success in explaining K- and L-shell excitation in collisions involving these shells.[3,4,20–28] The model is not so good an approximation for the description of outer electrons where the nuclear charges are more fully screened and the electron-electron interactions become more important. The dominance of the continuous portion of the electron energy spectra, which falls between 100 and 600 eV, implies that rapid mechanisms (10^{-16}–10^{-17} sec) at work during the collision (as opposed to Auger transitions in the separated ions after the collision) are responsible for most of the ionization that occurs. This conjecture is consistent with the Kr-Kr L Auger data of deGroot and co-workers[12,13] who conclude that for 0.5–1.6 MeV collisions 20 to 25 electrons are ionized from the collision complex before Auger emission takes place in the separated ions after the collision.

II. THE EXPERIMENTAL METHOD

The projectile Kr ions are produced in the terminal of a 2-MV Van de Graaff accelerator, mass analyzed and directed into a 42-cm diameter scattering chamber. The isotope ^{84}Kr (not always fully resolved from the lesser ^{83}Kr component of the beam) passes through a 0.76-mm aperture, the target gas region, and another 0.76-mm aperture. This latter aperture is on the axis of the annular collimator which defines the angle through which the scattered ions to be detected have been deflected. The target gas, either Kr or Xe, effuses from a 0.75-mm needle and the beam passes approximately 1 mm above the needle. The electrons are detected at 90° with respect to the beam direction after passing through two horizontal slits and a cylindrical electrostatic analyzer. The exit slit of the analyzer provides 5% energy resolution, a compromise between resolution and counting rates; and the electrons are detected with a channeltron-type electron multiplier. Two annular collimators define the scattering angle of those ions to be detected. Ions passing through these collimators strike a CuBe surface and secondary electrons from the impacts are directed into a second electron multiplier. Further experimental details and the criteria used to ensure single collisions may be found in Refs. 29 and 30.

With this apparatus, two types of data were obtained. First, noncoincident electron spectra were measured. For this the scattered ions were accumulated to a preset count after which the voltages on the electron analyzer were incremented to allow electrons of another energy to pass through the analyzer. For the coincidence data the counts from the electron detector were used as start signals for a time-to-amplitude (TAC) converter which was then stopped by any scattered ion counts arriving within a 5-μsec time window of a start pulse. Events correlated in time appear as a peak in the resulting TAC spectrum. Depending on the collision parameters, the time resolution (full width at half maximum) of the experiment was 50–100 nsec. With this experiment an electron of known energy can be associated with a collision whose scattering angle is known. The incident energy E_0 is also known and if an interatomic potential is assumed, the impact parameter and R_0 may be calculated for the collision which resulted in the ejection of that electron.[31,32]

III. EXPERIMENTAL RESULTS

A. Noncoincidence electron spectra

Figure 1 shows the doubly differential cross sections for the production of electrons with energies from 100 to 1500 eV in Kr-Kr collisions. The 0.2-, 0.4-, and 0.6-MeV data are from the work of Gordeev and co-workers[1,2] and the 1.2-MeV data of the present work have been normalized to Ref. 1 at 100 eV. The emission angle for Ref. 1 was 123° and is 90° for the present work. The dominant feature of these spectra is a continuum extending from 100 eV to approximately 700 eV; it is this continuum which is the subject of the present paper. Most of the electrons in the range of 800–1400 eV may be attributed to L-shell vacancy production and the subsequent filling of the vacancies by Auger decay. Figure 2 shows the continuum region in greater detail for incident ion energies from 0.13 to 2.0 MeV. Except for the suggestion of a shoulder between 100 and 250 eV, the predominant feature of these spectra is the structureless continuum extending to beyond 500 eV. This continuum cannot result from ordinary Auger processes because the usual Kr M-shell Auger processes result in electrons of fewer than 100 eV and those from L-shell vacancy production have much higher energies (Fig. 1). Similar results are observed for the Kr-Xe collisions; however, here it would be possible for M-shell vacancy production in the Xe targets to contribute to the spectra. These data are shown in Fig. 3, and Fig. 4 shows the 130-keV data on a linear scale together with a 2.0-MeV H^+-Xe spectrum from the work of Scherer.[33] It is observed that the proton-excited satellites extend in energy down to about 300 eV. In Xe-

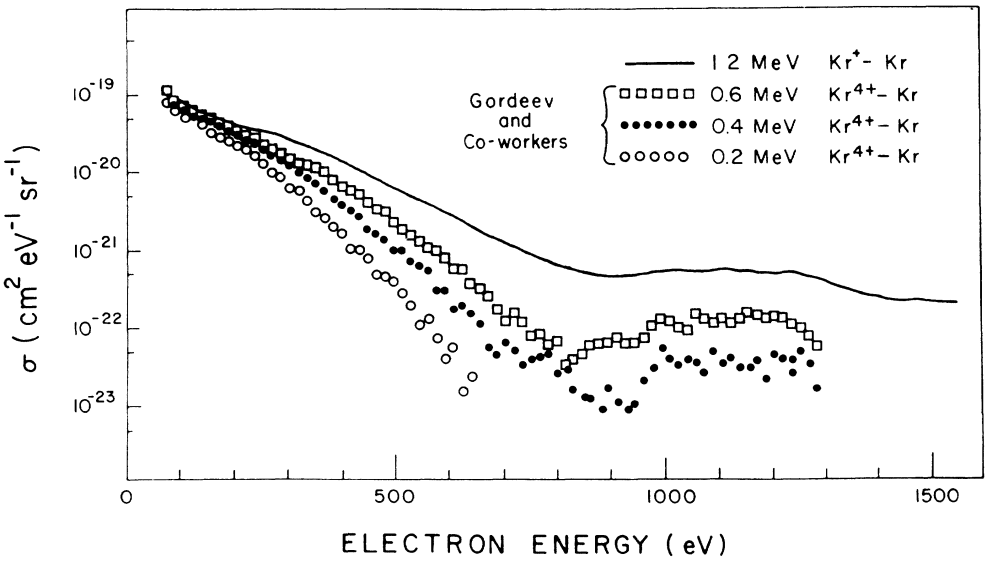

FIG. 1. Doubly differential cross sections for the production of electrons in Kr-Kr collisions. The present 1.2-MeV data have been normalized to those of Gordeev and co-workers (Ref. 1) at 100 eV. The continuum from 100 to 800 eV is the subject of the present paper. The peak between 900 and 1400 eV is the result of L-shell vacancy production.

Xe collisions where additional satellites are possible, electrons with energies from 250 to 500 eV dominate the spectrum.[34,35] These data indicate that while customary Auger electrons from Xe M-shell excitation may contribute to the Kr-Xe spectra presented here, they are unlikely to provide a major contribution to the region in question.

B. Coincidence electron spectra

For the Kr-Kr combination, coincidence data were obtained for incident ion energies from 150 keV to 1.6 MeV and for scattering angles in the range of 3°–10°. Figure 5 shows these data for the case of 3° scattering. In Figs. 5(a) and 5(b) the data show broad, but well-defined, peaks for electron energies between 100 and 400 eV. This is in contrast to the noncoincidence data of Fig. 2 which includes electrons from all possible impact parameters. As shown in Fig. 5(c), at higher collision energies the structure becomes less pronounced even though the numbers of electrons found in this energy range increases. Figure 6 shows similar data for Kr-Xe collisions for the case of 4° scattering and again, the data show a broad peak in the electron energy range of 100–400 eV. Figure 7 shows a more extensive data set, this time plotted on a logarithmic scale, for the 6° scattering data. Here it is observed that the character of the spectra changes in going from the 0.3-MeV to the 0.8-MeV data. Not only do the absolute numbers of electrons increase, but a higher percen-

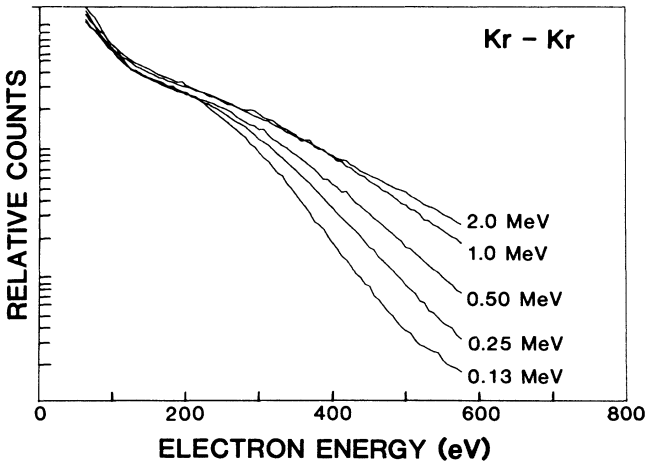

FIG. 2. Doubly differential data showing the relative numbers of electrons observed for selected values of the incident ion energies for Kr-Kr collisions.

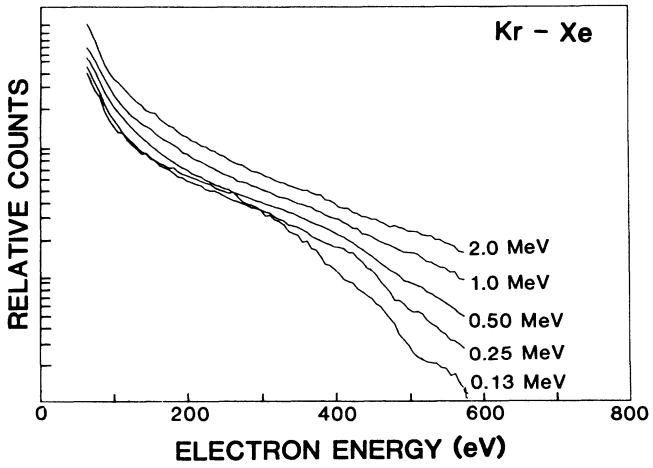

FIG. 3. Doubly differential data showing the relative numbers of electrons observed for selected values of the incident ion energies for Kr-Xe collisions.

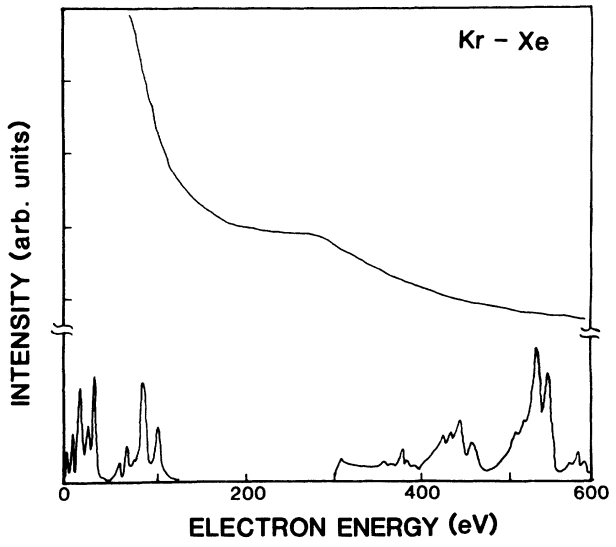

FIG. 4. A linear plot of the 0.13-MeV data from Fig. 3 together with data obtained by Scherer (Ref. 33) for 2.0-MeV H^+-Xe collisions.

tage of them fall in the 400–600-eV range for the higher-energy data sets.

In order to obtain relative cross sections for this continuum electron emission from the data in Figs. 5–7, it was necessary to perform a background subtraction to account for those low-energy electrons arising from other sources (e.g., autoionization of the outer shells). It was found that the low-energy portion of the spectra at and near threshold could be fitted reasonably well to an exponential tail. Figure 8 shows this estimated background for Kr-Kr data as a solid line and a similar figure may be found in Ref. 19 for the Kr-Xe data. The remaining area under each of these curves then represents those continuum electrons ejected from a collision having the impact parameter and R_0 associated with that energy and scattering angle. An internuclear potential must be assumed in order to calculate these collision parameters, and reasonable estimates are provided by either the potential suggested by Moliere[31] or the one by Bohr.[32] These screened Coulomb potentials provide R_0 values in good agreement with each other for collisions for which the innermost shells interpenetrate; however, for more gentle collisions where electron screening of the nuclei is important they differ considerably. For example, Shanker and co-workers[35] report that the Bohr potential overestimates the screening and results in a potential that is 30% too low (compared to the results of a Moliere-type potential) for internuclear distances corresponding to the M-shell radius for the Xe-Xe system. The R_0 values throughout this paper are calculated using the Moliere potential.

The areas representing the relative cross sections for continuum electron emission derived from the data in this way are shown in Figs. 9 and 10, where the error bars represent estimates of uncertainties in the subtraction of backgrounds. Both sets of data show two thresholds when plotted versus R_0. These thresholds appear at approximately 0.60 and 0.30 a.u. for the Kr-Xe data and at approximately 1.0 a.u. and a less distinct one at 0.5–0.6 a.u. for the Kr-Kr data. The open squares represent the present data and the closed circles in Fig. 9 represent data derived from the curves of Afrosimov and co-workers for collisions at 50 keV.[8] These latter data have been normalized to the present data at 0.65 a.u. (the closed squares). For each of these collision combinations the double threshold indicates that the continuum electrons observed in the coincidence measurements have

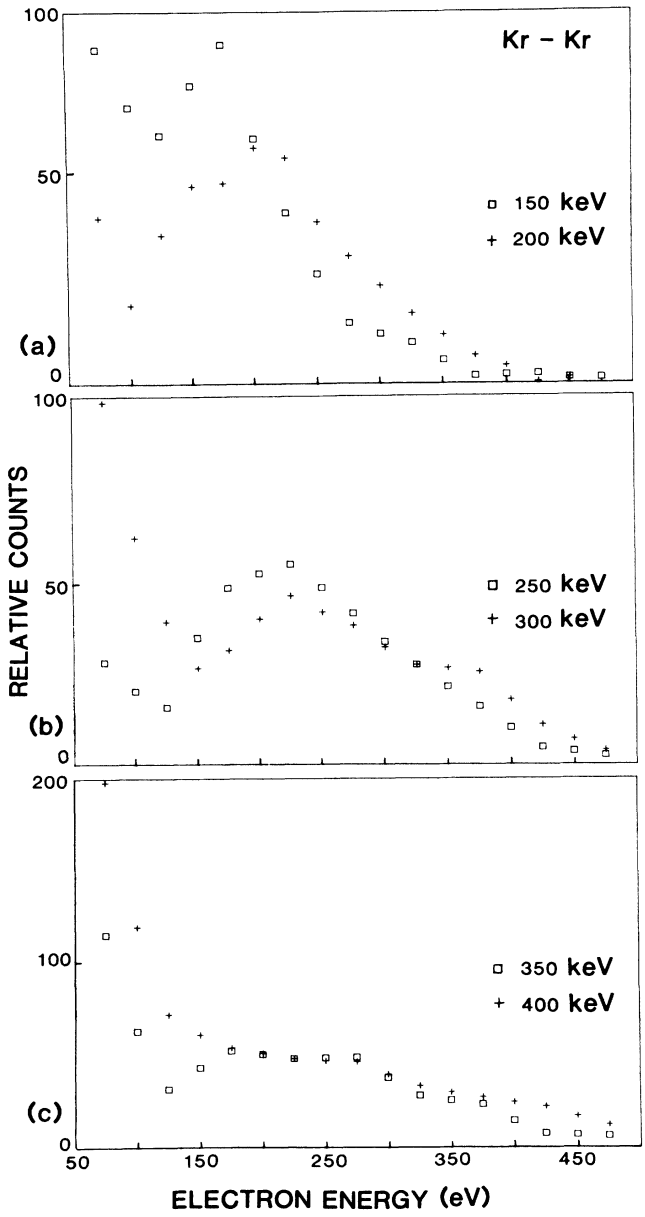

FIG. 5. Electron energy spectra obtained by detecting only those electrons ejected from Kr-Kr collisions for which the incident ion was scattered through 3°.

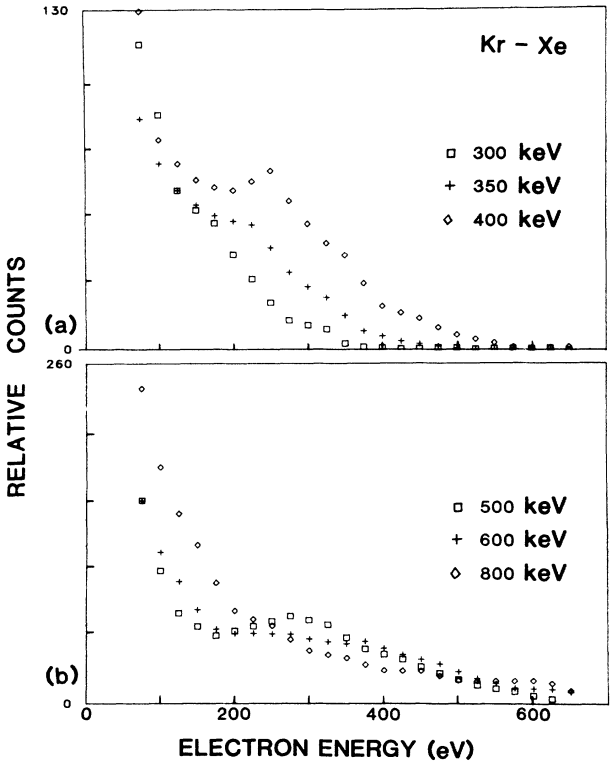

FIG. 6. Electron energy spectra obtained by detecting only those electrons ejected from Kr-Xe collisions for which the Kr ion was scattered through 4°.

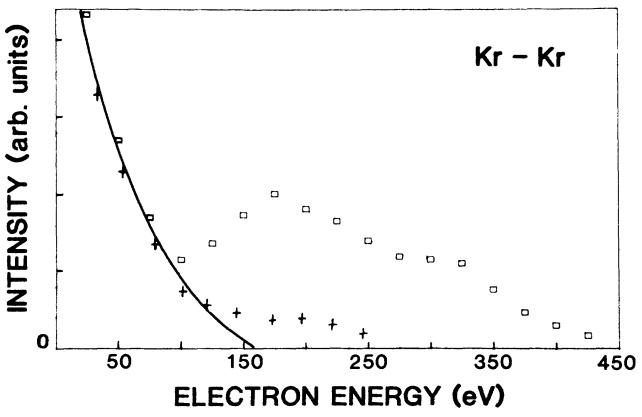

FIG. 8. Kr-Kr data obtained near threshold showing the low-energy fit to the exponential tail used for the background subtraction.

their origin in two different excitations each having a different impact parameter dependence.

In summary, both sets of data show the following features: There is an impact-parameter dependence for the emission of electrons, but the emitted electrons display a continuous range of energies. For the Kr-Kr spectra, ordinary Auger processes cannot account for the electron energies observed; for the Kr-Xe spectra, it is possible that Xe M electrons from ordinary Auger processes might contribute to the spectra, but they are not likely to be the dominant factor in the nearly featureless coincidence spectra. Ionization and inelastic energy-loss

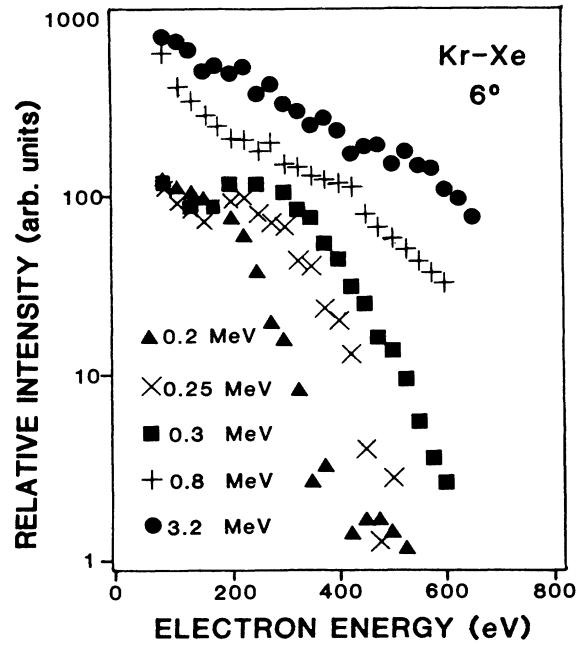

FIG. 7. Data similar to those of Fig. 6 except for 6° scattering and plotted on a semilogarithmic scale.

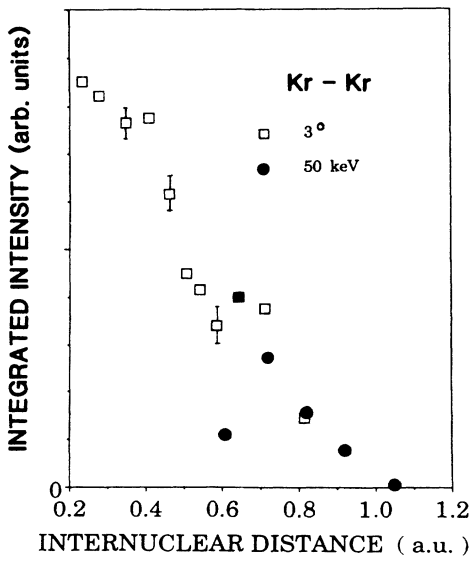

FIG. 9. The areas under curves like those in Fig. 5 plotted versus the collisions' distances of closest approach for Kr-Kr collisions. The 3° data are from the present work and the 50-keV data are from Ref. 8. These data sets have been normalized to each other at 0.65 a.u. (the closed square symbol).

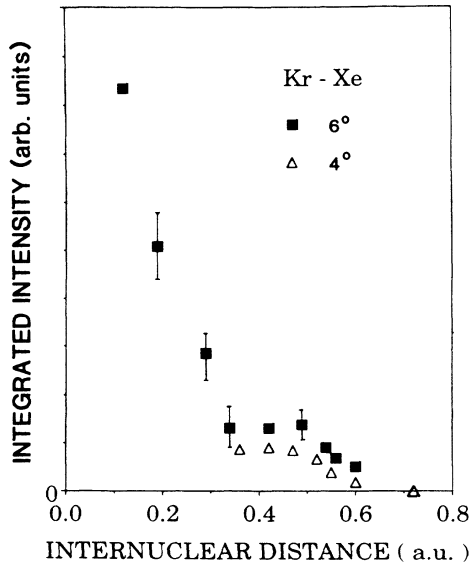

FIG. 10. The areas under curves like those in Figs. 6 and 7 plotted versus the collisions' distances of closest approach.

data for Kr-Kr and Kr-Xe collisions are also available for the present range of impact parameters.[10] In these earlier data the R_0-dependent structure is better resolved for the Kr-Xe collisions than for the Kr-Kr collisions. For this reason the Kr-Xe data will be discussed first.

IV. DISCUSSION

The excitation thresholds which are observed when the data are plotted versus the collisions's R_0 values suggest that the molecular orbital model proposed by Fano and Lichten[3,4,20–22] may be used to explain some aspects of these collisions. Whereas the molecular potential curves proposed by Fano and Lichten were dynamic MO's formed during the collision and called diabatic MO's, adiabatic molecular potential curves serve as a useful starting point for the discussion. Figure 11 shows the adiabatic curves as calculated by Eichler and coworkers[22] for the Kr-Xe system. The nomenclature for these curves is arrived at by counting up from the lowest level for each angular momentum state, i.e., $1\sigma, 2\sigma, 3\sigma, \ldots, 1\pi, 2\pi, \ldots$. Because of the noncrossing rule, this leads to a fairly simple labeling system. On the

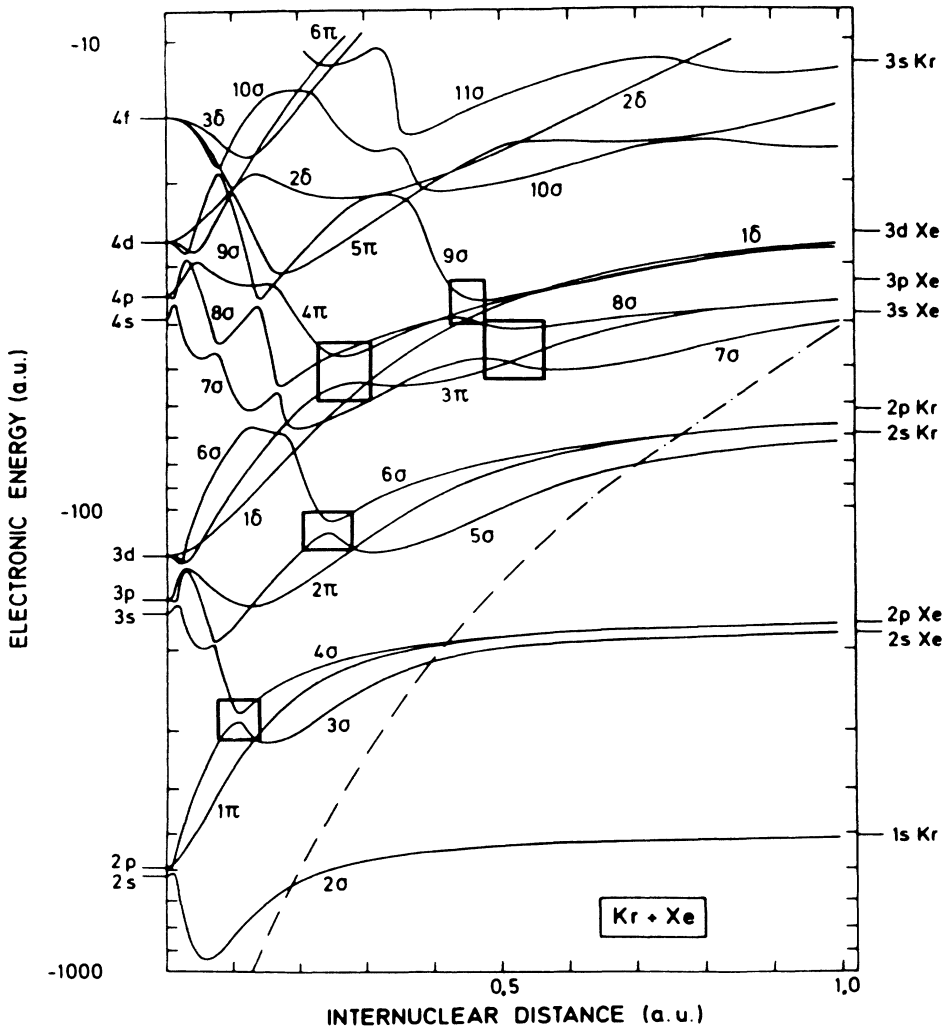

FIG. 11. Molecular-level diagram for the Kr-Xe system (from Ref. 22).

other hand, this is not a practical way to identify the diabatic MO curves used in the Fano-Lichten model, and they used the united-atom designation for the specification of their dynamic MO's. For example, in Fig. 11 the diabatic $4f\sigma$ MO is that orbital which connects the united-atom $4f$ level with the separated-atom Kr $2s$ level through the series of avoided crossings of the adiabatic $5\sigma, 6\sigma, \ldots, 10\sigma$ levels. This is physically appropriate because radial coupling, due to the relative motion of the two nuclei, makes it highly likely that an electron's energy will be best described by the $4f\sigma$ curve. Wherever necessary for clarity, both designations will be given in this paper.

A. Kr-Xe collisions

The data in Fig. 10 show excitation thresholds for this continuum electron production at 0.3 and 0.6 a.u. The 0.3-a.u. threshold is seen to correspond to the series of avoided crossings in Fig. 11 which make up the diabatic $5g\sigma$ level (originating with the Xe $3s$ level and being promoted through sections of the $7\sigma, 8\sigma, 9\sigma, \ldots$ adiabatic levels). Electrons promoted by this MO (or correspondingly, vacancies demoted by this MO) leave holes which may be filled by either radiative or radiationless decay. The latter process will ordinarily be the faster one and will result in the ejection of electrons from the system. If these electrons are emitted after the nuclei are well separated, the electron energies may correspond to normal Auger energies, or more likely, satellites of Auger lines because of the multiple ionization caused by the collision. On the other hand, a decay before the atoms are well separated will result in a broadening of what might otherwise have been a fairly narrow, discrete Auger line. In the present example, the promotion of a $3s$ electron from Xe, and the filling of the 7σ level at its lowest point would mean that more than 1300 eV would be available for the electronic excitation process. Because this is more than twice the energy that would be available if the decay were to take place in the separated atom after the nuclei were far apart, it is seen that a wide range of noncharacteristic energies might be present in the energy spectrum of the emitted electrons.

The curves in Fig. 11 do not extend to where they may be used for a discussion of the threshold at 0.6 a.u. The Fano-Lichten model and the curves calculated by Eichler and co-workers were for the interpretation of inner-shell excitations for which the Born-Oppenheimer approximation is valid and the primary force influencing the motion of the electrons is that of the poorly shielded nuclei. As one moves toward the outer shells ($n = 3$ or 4), the shielding becomes more complete, the electron velocities comparable to the nuclear velocities, and the model is expected to become a poorer approximation.[3,4,22] However, the presence of a threshold at 0.6 a.u. in Fig. 10 suggests that some aspects of the MO model may still be useful in describing collisions where shells other than the innermost shells are involved. For this reason these calculations have been extended to the region in question and the results are shown in Fig. 12. The series of avoided crossings between 0.3 and 0.4 a.u. which couple the MO's to continue the diabatic $5g\sigma$ level originating in the separated-atom $3s$ level of Xe (Fig. 11) are very pronounced. In addition, there is another series of avoided crossings between 0.6 and 0.8 a.u. It is to this promotion that we attribute the 0.6-a.u. threshold in the data of Fig. 10. Electrons from a large number of separated-atom levels in either collision partner may be excited through this promotion. Even within this one-electron framework, the multiplicity of possible excitations and ionizations could lead to a continuum in the spectra of emitted electrons. Certainly, should the vacancies be filled during the collision, when the MO's are changing with internuclear distance, the resulting electrons would have a continuous range of energies. Furthermore, in dealing with the MO's calculated for these outer electrons the adiabatic curves are not realistic. The close spacing of the outer levels and the velocities under consideration here couple and broaden these levels and make it impossible to assign well-defined energies to outer electrons during a collision. The likelihood of multiple-electron transitions might also contribute to the continuum nature of the ejected electron spectra.[36,37] For example, two electrons may be promoted by a σ MO and as soon as the promoted electrons move halfway toward the energy continuum, it is energetically possible for an autoionization to occur. To summarize, the promotions shown in Fig. 12 originate in MO's which are tightly enough bound to be reasonably well-

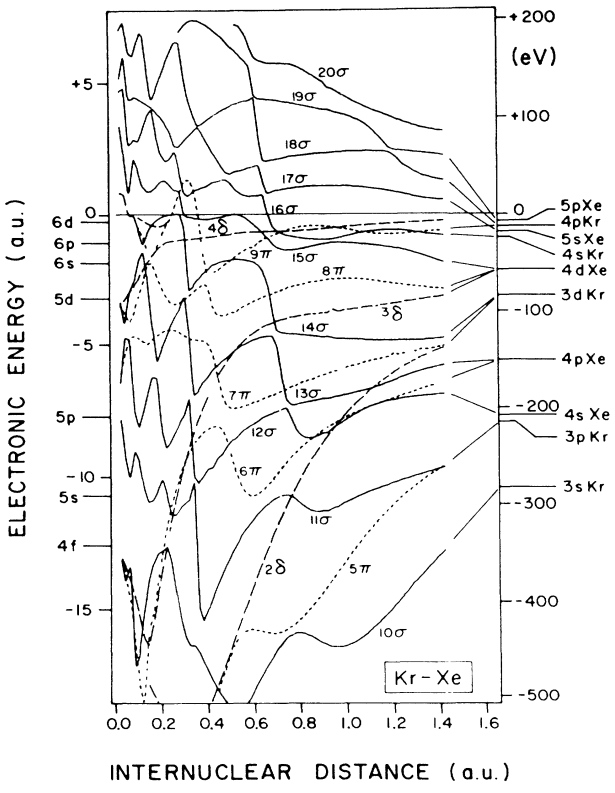

FIG. 12. An extension of the Kr-Xe calculations of Fig. 11 (from Ref. 19).

described by the one-electron MO model and these correspond well to the experimental thresholds in Fig. 10. Even though the one-electron description cannot be applied quantitatively to the outer shells, it does serve as a framework within which to discuss various mechanisms for the production of continuum electrons.

These excitation thresholds have also been observed in a related experiment in which the ionization of the scattered Kr ion was measured as well as the inelastic energy loss Q for the collision as a whole.[10] For collisions having R_0 values decreasing from 0.6 to 0.4 a.u., the average charge state of the scattered Kr ion increases from 1 to 5. The Q value for these collisions is less than 1 keV, which must include the energy required to ionize any electrons from the Xe target as well (the final Xe charge state was not measured in Ref. 10). In the range from 0.4 to 0.2 a.u., another three electrons, on the average, are removed from the Kr ion, but here the Q value increases by approximately 2.5 keV. These two excitations, the latter one requiring a great deal more energy, are consistent with the data in Figs. 7 and 10 and the interpretation that these thresholds corresponds to the onset of excitations due to the promotions illustrated in Fig. 12.

B. Kr-Kr collisions

Prior research into this system[8,38–40] has uncovered a number of individual excitations, often poorly resolved. For collisions having R_0 values in the 0.8–1.0-a.u. range, the average scattered charge state increases by about one and inelastic energy-loss measurements by Fastrup and Hermann[38] show that two $3d$ vacancies are produced (on

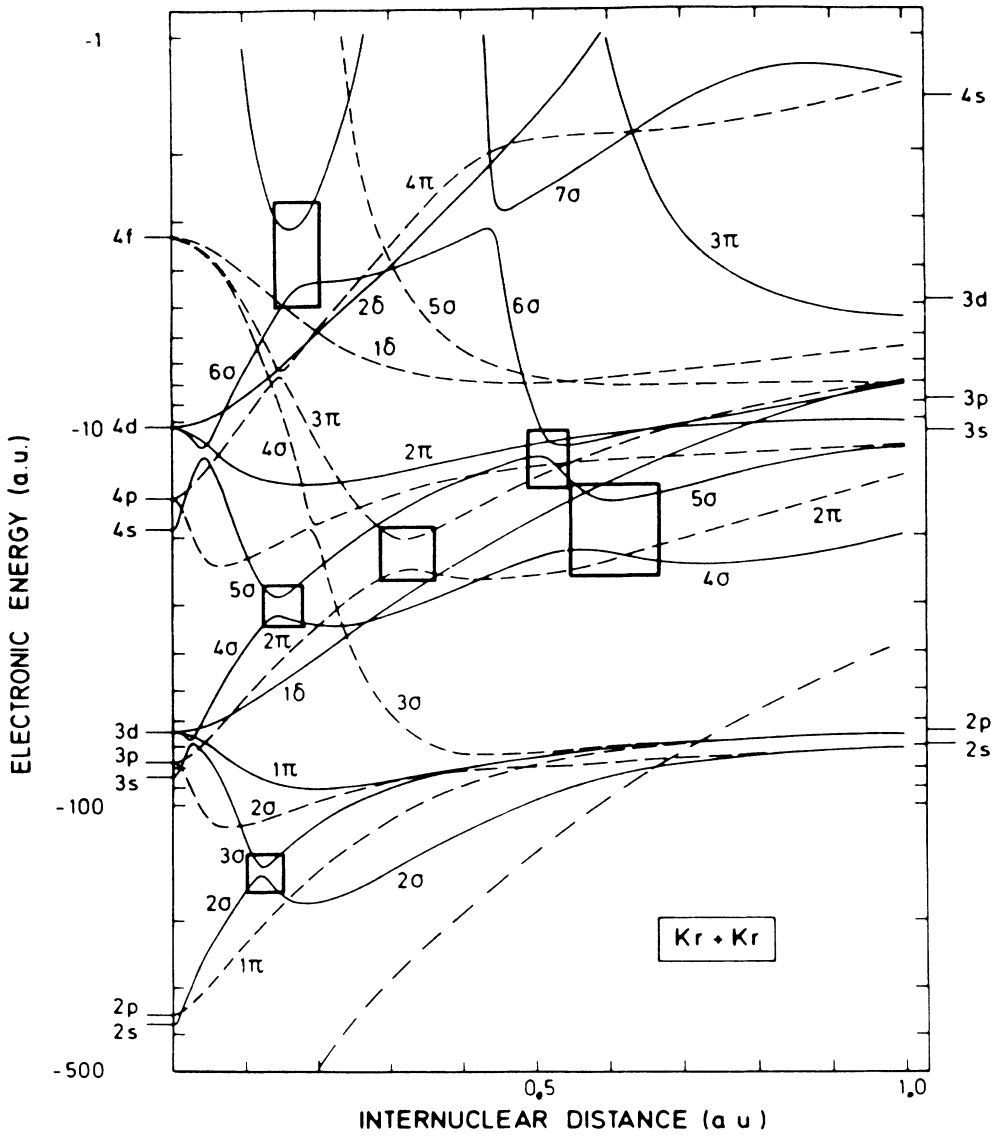

FIG. 13. Molecular-level diagram for the Kr-Kr system (from Ref. 22).

the average, one in each ion). The MO diagrams for this system are shown in Figs. 13 and 14, and Fig. 14 shows that the excitation observed by Fastrup and Hermann is consistent with the promotion of two electrons along the 6σ *ungerade* level connecting with the separated-atom $3d$ level in Fig. 14. It appears that it is the excitation which is responsible for the 1.0-a.u. threshold of the data in Fig. 9. The second threshold correlates well with the $4\sigma, 5\sigma, 6\sigma \ldots$ *gerade* promotion at 0.6 a.u. These excitations are also observed in the ionization data of Ref. 9 (which used the Bohr, rather than the Moliere potential, resulting in threshold values of 0.8 and 0.6 a.u.). Between R_0 equal to 1.0 and 0.6 a.u. the average scattered charge state increases by 2.5 and the inelastic energy-loss for this excitation is approximately 1.2 keV.[10] It has been shown for other symmetric systems that the average charge of the recoil ion usually equals that of the scattered ion for collisions of this type,[16,41] implying that for the excitation under consideration it takes approximately 200–300 eV for each electron's removal. This number is in good agreement with the electron energies shown in Fig. 5.

The discussion so far has concerned itself with the excitation process. It is the deexcitation process which results in the ejection of electrons with energies which are not characteristic of separated-atom energy levels. These noncharacteristic energies may be attributed to decay during the collision. For example, should a vacancy be present in the gerade 4σ level (Fig. 14), more than 500 eV of energy might be available for the process, depending upon where along the path the decay takes place. As processes such as this, together with collision broadening of the outer levels, are probably the cause of the continuous nature of the electron spectra presented here, one must conclude these electrons are ionized during the collision rather than in well-separated ions after the collision. This in turn, based on velocities and internuclear distances, requires decay times of 10^{-16}–10^{-17} sec. These unusually short times may be due to dynamic processes during the collision; on the other hand, Hahn has found certain decay processes in isolated Ar ions to be this rapid.[42] The data in Fig. 1 and Refs. 11–13 do show that rapid processes during the collision remove many more electrons than do Auger processes in the separated atom.

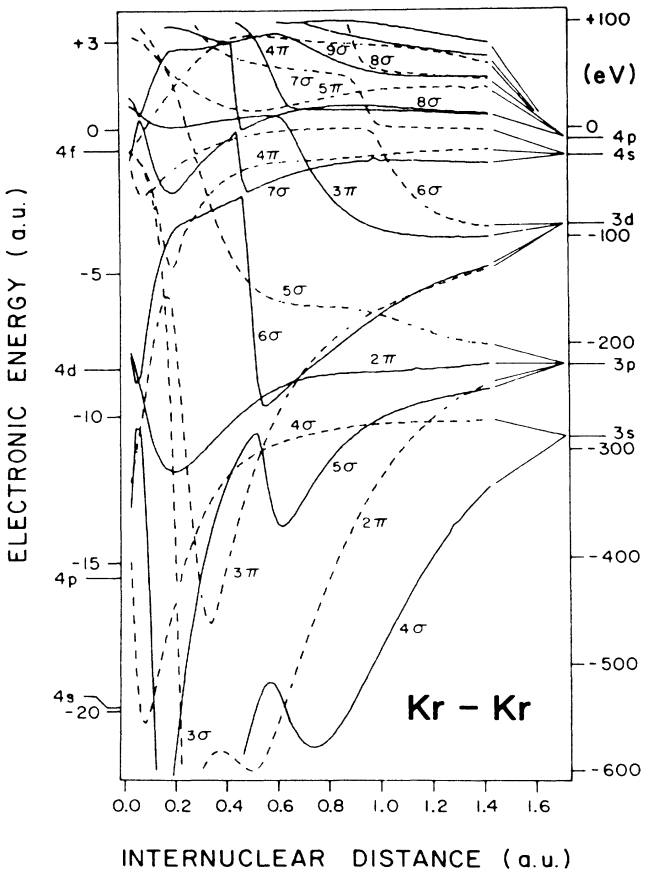

FIG. 14. An extension of the Kr-Kr calculations of Fig. 13 (from Ref. 18).

It is not clear whether or not the "molecular excitation," or promotion to the continuum proposed by Schiwietz and co-workers[14] for lower-energy (0–110 eV) electrons emitted from the Ar-Ar system plays a significant role here; however, the higher electron energies of the present spectra suggest not. Another suggestion has been made for the origin of these continuum electrons; however, it is not consistent with the calculations of Figs. 13 and 14. Without having direct knowledge of the impact parameter dependence for the production of these electrons Gordeev and co-workers[1] pointed out that the filling of the diabatic $4p\pi$ MO (connecting the separated-atom $4s$ state to the united-atom $4p$ state via the 4π and 3π *ungerade* curves) during the collision could account for the range of electron energies observed. This MO drops rapidly in energy as R_0 decreases below 0.4 a.u., but it does not become low enough to account for the observed electron energies until R_0 falls below 0.2 a.u. The present impact parameter dependent data and its interpretation are consistent with the Eichler-Wille calculations of Figs. 13 and 14. Afrosimov and co-workers[8] used their data, together with the assumption that it is the decay of the diabatic $4p\pi$ MO that is responsible for the continuum electrons, to derive experimental values for the orbital which would be consistent with their interpretation. In addition to this controversy, interpretations have been made which utilize interference effects based on the filling of the $4p\pi$ MO on the incoming and outgoing collision paths.[5,8] The present data do not show interference effects and do not support these interpretations. Furthermore, recent attempts to repeat the experiment of Ref. 5 under conditions identical to those in Ref. 5 have failed to observe the effect.[7]

V. SUMMARY

The experiment observed a continuum in the range of 100–600 eV in the emitted electron energy spectrum following both Kr-Kr and Kr-Xe collisions. Further, the experiment determined the impact-parameter dependence

for this emission and the data show definite thresholds for the continuum electron production when plotted versus the collision's distance of closest approach. The existence of these thresholds encourage an interpretation within the framework of the MO model proposed by Fano and Lichten, even though the collision parameters and the electron shells involved place the data beyond the usual region of applicability of this one-electron model. Where the model is expected to hold, it is in good agreement with the observed thresholds. The data imply that mechanisms with decay times of 10^{-16}–10^{-17} sec dominate the ionization process for these heavy ion-atom combinations and result in most of the electrons being removed during collision. Exactly what these mechanisms are is unclear, but fast Auger-type decays (not necessarily limited to two-electron interactions) taking place during the collision would be consistent with the electron energies observed.

ACKNOWLEDGMENTS

The calculations shown in Figs. 12 and 14 were carried out by Dr. Kennedy J. Reed. The authors are also indebted to Professor Arnold Russek for helpful conversations and to Peter de Groot and Michael Zarcone for help in obtaining a portion of the data. This research was supported by the National Science Foundation under Grants Nos. PHY8705501 and PHY8818347.

[1]Yu. S. Gordeev, P. H. Woerlee, H. de Waard, and F. W. Saris, J. Phys. B **14**, 513 (1981).
[2]P. H. Woerlee, Yu. S. Gordeev, H. de Waard, and F. W. Saris, J. Phys. B **14**, 527 (1981).
[3]U. Fano and W. Lichten, Phys. Rev. Lett. **14**, 627 (1965).
[4]W. Lichten, Phys. Rev. **164**, 131 (1967).
[5]D. Liesen, A. N. Zinoviev, and F. W. Saris, Phys. Rev. Lett. **47**, 1932 (1981).
[6]A. P. Shergin, R. Stotzel, Z. Roller, R. Bilau, and H. O. Lutz, Phys. Rev. A **34**, 4490 (1986).
[7]R. Koch, S. Kelbch, and Horst Schmidt-Bocking, Phys. Lett. **127**, 347 (1988).
[8]V. V. Afrosimov, G. G. Meskhi, N. N. Tsarev, and A. P. Shergin, Zh. Eksp. Theor. Fiz. **84**, 454 (1983) [Sov. Phys.—JETP **57**, 263 (1983)].
[9]B. Fricke and W-D Sepp, J. Phys. B **14**, L549 (1981).
[10]A. A. Antar and Q. C. Kessel, Phys. Rev. A **29**, 1070 (1984).
[11]P. deGroot, M. J. Zarcone, and Q. C. Kessel, Nucl. Instrum. Methods Phys. Res. B **24/25**, 159 (1987).
[12]P. deGroot, M. J. Zarcone, and Q. C. Kessel, Phys. Rev. A **36**, 2968 (1987).
[13]P. deGroot, M. J. Zarcone, and Q. C. Kessel, Phys. Rev. A **38**, 3286 (1988).
[14]G. Schiwietz, B. Skogvall, J. Tanis, and D. Schneider, Phys. Rev. A **38**, 5552 (1988).
[15]Q. C. Kessel, A. Russek, and E. Everhart, Phys. Rev. Lett. **14**, 484 (1965).
[16]Q. C. Kessel and E. Everhart, Phys. Rev. **146**, 16 (1966).
[17]R. Anholt, Rev. Mod. Phys. **57**, 995 (1985).
[18]P. Clapis, R. Roser, K. J. Reed, and Q. C. Kessel, Nucl. Instrum. Methods Phys. Res. B **10/11**, 104 (1985).
[19]P. Clapis, R. Roser, K. J. Reed, and Q. C. Kessel, Phys. Rev. Lett. **55**, 1563 (1985).
[20]M. Barat and W. Lichten, Phys. Rev. A **6**, 211 (1972).
[21]J. Eichler and U. Wille, Phys. Rev. A **11**, 1973 (1975).
[22]J. Eichler, U. Wille, B. Fastrup, and K. Taulbjerg, Phys. Rev. A **14**, 707 (1976).
[23]P. H. Woerlee, R. J. Fortner, S. Doorn, Th. P. Hoogkamer, and F. W. Saris, J. Phys. B **14**, L425 (1978).
[24]K. J. Reed, J. D. Garcia, and R. J. Fortner, Phys. Rev. A **22**, 903 (1980).
[25]Q. C. Kessel and B. Fastrup, Case Stud. At. Phys. **3**, 137 (1973).
[26]J. D. Garcia, R. J. Fortner, and T. M. Kavanagh, Rev. Mod. Phys. **45**, 111 (1973).
[27]W. Meyerhof and K. Taulbjerg, Annu. Rev. Nucl. Sci. **27**, 279 (1977).
[28]U. Wille and R. Hippler, Phys. Rep. **132**, 129 (1986).
[29]R. Rubino, M. S. thesis, University of Connecticut, 1985 (unpublished).
[30]P. Clapis, Ph.D. thesis, University of Connecticut, 1985 (unpublished).
[31]G. Moliere, Z. Naturforsch **29**, 133 (1947).
[32]E. Everhart, G. Stone, and R. J. Carbone, Phys. Rev. **99**, 1287 (1955).
[33]E. Scherer, Ph.D. thesis, University of Dortmund, 1980 (unpublished).
[34]A. Antar, P. Clapis, J. Gianopoulos, D. Olson, R. Rubino, G. Thomson and Q. C. Kessel (unpublished).
[35]R. Shanker, R. Hippler, U. Wille, and H. O. Lutz, J. Phys. B **15**, 2041 (1982).
[36]T. A. Carlson and M. O. Krause, Phys. Rev. Lett. **11**, 390 (1965).
[37]M. O. Krause and T. A. Carlson, Phys. Rev. **149**, 52 (1966).
[38]B. Fastrup and G. Hermann, Phys. Rev. A **3**, 1955 (1971).
[39]V. V. Afrosimov, Yu. S. Gordeev, M. N. Panov, and N. V. Fedorenko, Zh. Tekh. Fiz. **36**, 123 (1966) [Sov. Phys.—Tech. Phys. **11**, 89 (1966)].
[40]M. P. McCaughy, E. J. Knystautas, and E. Everhart, Phys. Rev. **175**, 14 (1968).
[41]E. Everhart and Q. C. Kessel, Phys. Rev. **146**, 27 (1966).
[42]Yukap Hahn (private communication).